3.3 ADVANCED CHARACTERIZATION OF IRRADIATION DEFECTS IN SILICON CARBIDE: POSITRON ANNIHILATION SPECTROSCOPY

— X. Hu, T. Koyanagi, Y. Katoh (Oak Ridge National Laboratory)

OBJECTIVE

This report describes the advanced characterization of irradiation defects in SiC using positron annihilation spectroscopy for better understanding of the microstructure and material properties in fusion environments.

SUMMARY

Positron annihilation spectroscopy (PAS), i.e., positron annihilation lifetime spectroscopy and coincidence Doppler broadening, was used to characterize the small vacancy clusters in 3C-SiC subject to various neutron irradiation conditions by capturing the dependence of irradiation temperature (380~800°C) and dose (0.01~30dpa). The vacancy cluster distribution obtained from PAS investigation is critically important to complement the current understanding of the microstructural evolution in SiC under the abovementioned neutron irradiation conditions, due to the cluster invisibility in TEM characterization. Subsequently, the vacancy clusters are then linked to the measured swelling behavior to provide insight into the correlation between microstructure and physical properties of SiC.

PROGRESS AND STATUS

Introduction

Silicon carbide (SiC) based-materials are attractive candidates for structural components in fusion reactor due to their superior irradiation tolerance. Swelling and irradiation creep are key properties in assessing the performance of SiC in nuclear service. Correlation between these properties and microstructural evolution has been studied for various irradiation conditions using conventional transmission microscopy (TEM) [1]. However, the irradiation response at the atomic scale is still poorly understood; TEM-visible defects can account for only a small fraction of swelling and irradiation creep [2]. In addition, understanding the elemental composition (chemistry) of the defect clusters is very limited, even for TEM-visible defects.

In this task, we will capture the TEM-invisible (conventionally) defects and characterize elemental composition of the defects in neutron-irradiated SiC using positron annihilation spectroscopy (PAS). PAS is powerful tool to detect atomic-scale vacancy-type defects. Additional experiments using Raman spectroscopy and synchrotron X-ray diffraction are also planned. This study will provide both new approaches to characterizing irradiation defects at the atomic scale, and a more detailed understanding of irradiation response of SiC. This will help guide the building of mechanistic models of the material properties and give a better understanding of a pathway toward to improving the irradiation resistance of SiC materials.

This report describes the system development of positron annihilation spectroscopy in ORNL along with the preliminary results of PAS investigation on neutron irradiated SiC.

Development of positron annihilation spectroscopy system

A PAS system was established within the Low-Activation Materials Development and Analysis (LAMDA) Lab at ORNL for this work, dedicated to investigating radiological materials. The system consists of two sub-techniques: positron annihilation lifetime spectroscopy (PALS) and coincidence Doppler broadening (CDB). A schematic diagram of this system is shown in Figure 1.

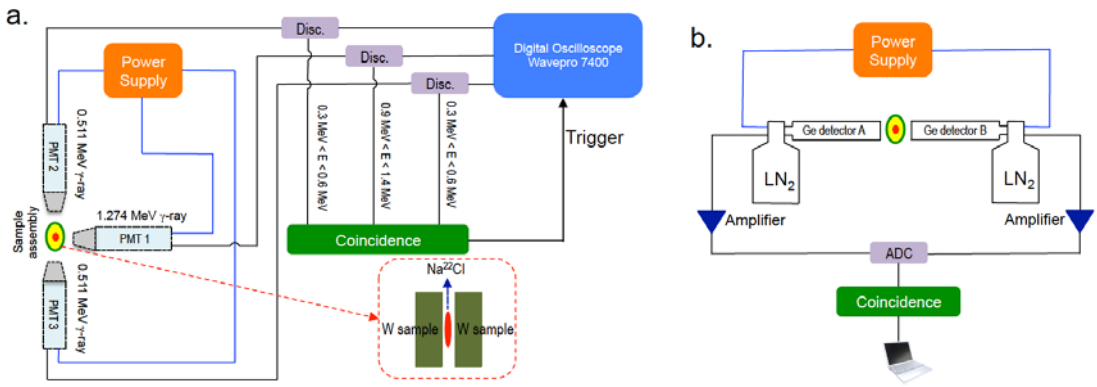

Figure 1. Schematic diagram of the PAS system: (a). Positron annihilation lifetime spectroscopy. (b). Coincidence Doppler broadening. The inset in (a) indicates the sample/source packing structure.

Measurement of positron lifetimes of the samples of interest was performed using the system shown in Figure 1 (a), at room temperature, using a conventional sample-source-sample sandwich geometry (The sample packing structure is also shown in Figure 1 (a)). The positron source was made from a ^{22}NaCl solution directly evaporated onto the surface of the samples with an intensity of 740 kBq. The stack of two identical samples was wrapped by thin aluminum foils to form a sample assembly. The 1.274 MeV gamma ray, indicating a positron emission event, and the two 0.511 MeV annihilation gamma rays were detected using fast scintillators (BaF_2) coupled with photomultiplier tubes (PMTs). Unlike in a traditional experimental setup, a double-stop setup was employed in this work. Pairs of 0.511 MeV gamma rays were detected by two PMTs (PMT 2 and PMT 3) placed face-to-face on the opposite sides of the source-sample assembly. The positron lifetime is defined as the average value of the time intervals between the birth gamma ray and the two annihilation gamma rays for a coincidence event (10 ns). Data were obtained using a LeCroy® digital oscilloscope with a calculated system timing resolution of 140 ps. Each recorded lifetime spectrum contained a total of ~1×10^6 counts and was analyzed by three components, i.e., as a sum of exponentials after deconvolution of the experimental resolution function—usually approximated as a Gaussian function.

Positrons eventually are annihilated by electrons, producing predominantly two gamma rays traveling in approximately opposite directions, as is necessitated by energy-momentum conservation during annihilation. Since there is a net center of mass energy associated with the annihilating positron-electron pair, the total energy does not split equally for the two gamma rays. One gamma ray is upshifted and the other is downshifted. The energy shift of each photon is given by

$$\Delta E = \frac{1}{2} p_L c = \frac{1}{2} \theta_L m_0 c^2 \quad , \qquad (1)$$

where ΔE is the photon energy difference from the nominal value, p_L is the corresponding longitudinal momentum shift along the direction of gamma ray emission, in atomic unit (1 a.u.=7.28 mrad×$m_0 c$), θ_L is the angular deviation of the photons from 180°. Since p_L has element-specific spectral distributions that correspond to the momentum distributions of the annihilation electrons, analysis of the orbital electron momentum spectrum (OEMS) provides information on the local chemical environment where the positron annihilates. The OEMS is typically represented as the fraction of annihilations at each momentum interval as a function of p_L, normalized by a standard spectrum. It is more convenient to represent OEMS data in so called *S*−*W* plots. The *S* is a fraction of the low-momentum annihilation defined by the specified p_L region, which in this study is $p_L \leq 0.382\, a.u.$ The *W* is the corresponding high-momentum annihilation fraction, defined as $1.0\, a.u. \leq p_L \leq 4.0\, a.u.$. A particular microstructure produces a point on an *S*−*W* plot. *S*−*W* correlation plots are useful in detecting the change in the nature of the positron trapping defects, since the slope of the plot is a fingerprint of a specific vacancy [3].

The CDB setup is shown in Figure 1 (b). Both annihilation gamma rays are detected in coincidence by using two HPGe detectors facing the source-sample sandwich from opposite sides. The CDB measurement was performed simultaneously with PALS by using the same sample-source assembly. The coincidence events falling within a selected window $2m_0c^2 - 2.0\ keV < (E_1 + E_2) < 2m_0c^2 + 2.0\ keV$ were collected for data analysis to obtain a low-background Doppler broadening annihilation spectrum with a peak-to-background ratio of better than 10,000:1.

Evaluation of irradiated SiC materials

High-purity 3C-SiC monoliths were used in this study. Neutron irradiation was performed in the High Flux Isotope Reactor at ORNL. The specimens were irradiated at 380 ~ 800°C to 0.01 ~ 30 dpa. Assuming that 1 dpa in SiC is equivalent to 1×10^{25} n/m^2 (E > 0.1 MeV), the damage rate for neutron irradiation is ~5×10^{-7} dpa/s. The neutron irradiation conditions of the studied specimens are listed in Table 1.

Table 1. Specimen matrix for PAS experiment

Capsule ID	Irradiation temperature [°C]	Fluence [dpa]
Reference	Unirradiated	Unirardiated
T8A1	380	0.01
T8A2	380	0.11
TTN01	380	1.5
TTN03	440	31
T8B1	540	0.01
T8B2	540	0.1
TTN05	500	29
T8D1	790	0.1
T8E1	760	1.4
TTN07	750	29

Results

Positively charged vacancies create a long-range repulsive Coulomb potential, hence have small trapping probability and should not be detected by PAS. Therefore, carbon vacancy in SiC will not be captured in this study. Neutral and negative vacancies (i.e., complexes of Si-C and silicon vacancy), on contrary, can be detected and distinguished. To illustrate directly the influence of neutron irradiation on the measured positron lifetime data, Figure 2 plots the normalized spectra obtained for neutron irradiated SiC. Figures 2 (a), (b), and (c) demonstrate the irradiation dose dependence on the measured positron lifetime spectra at three different irradiation temperatures. The long-lifetime parts of the spectra became more intense with increasing radiation damage level, when comparing T8A1, T8A2, TTN01, and TTN03 (irradiated at 380~440°C). Same conclusions can also be drawn for the specimens irradiated at 500~540°C and 760~800°C. It is noted that the spectra was difficulty to distinct when irradiation dose is less than 1.5 dpa and 30 dpa irradiation leads to more significant long-lifetime tail shift. Figures 2 (d) and (e) show the irradiation temperature dependence on the measured positron lifetime spectra at ~ 0.1 and ~ 30 dpa, respectively. As to the low dose irradiation, the lifetime spectra overlapped, implying the insignificant damage evolution, even at 760~800°C, which is considered as the initial point for vacancy mobility. However, when the damage level reaches 30 dpa, the high temperature irradiation does enhance the long-lifetime parts by driving the formation of larger vacancy clusters, as shown in Figure 2 (e).

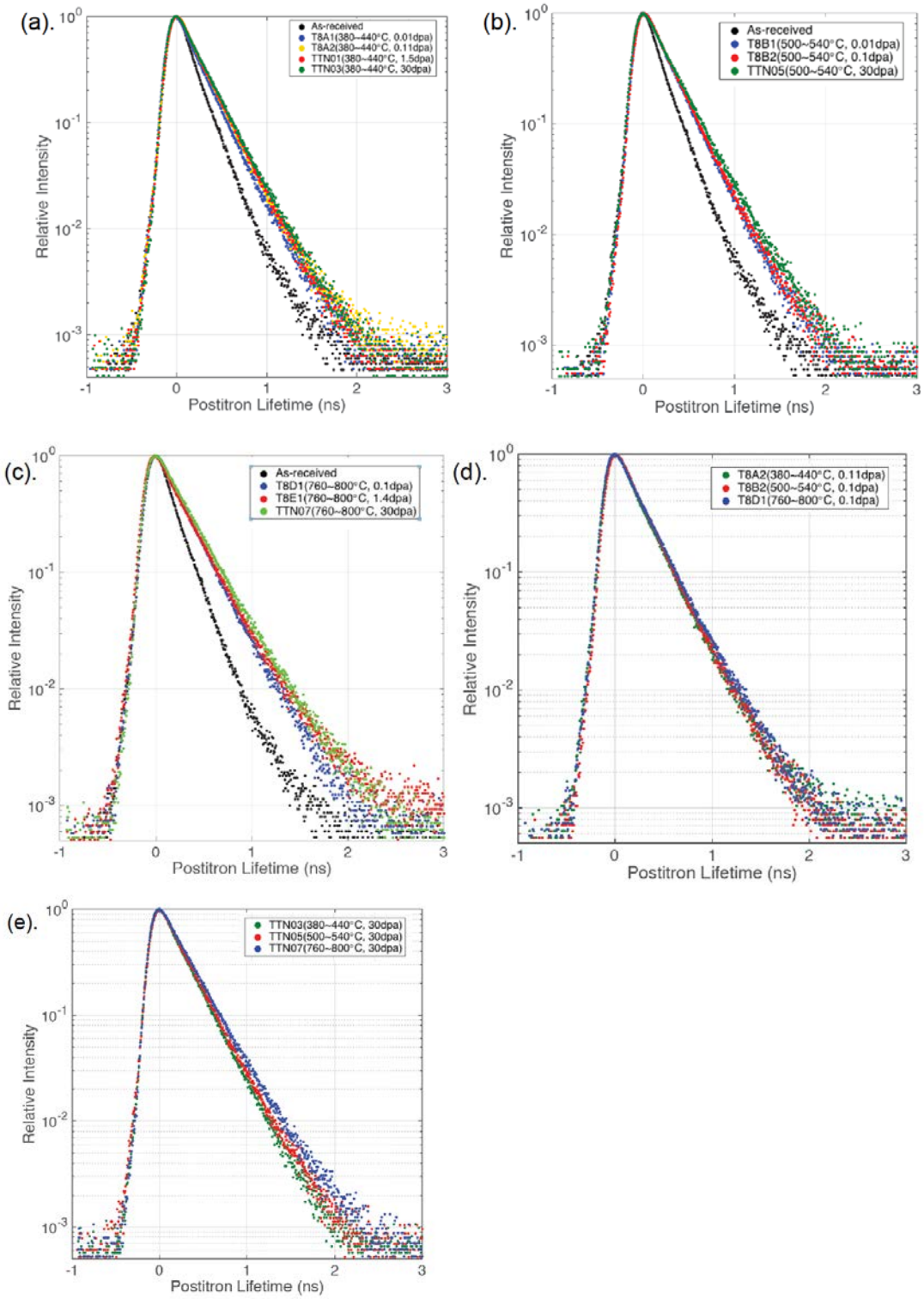

Figure 2. Normalized positron lifetime spectra of SiC exposed to various neutron irradiation conditions. (a), (b), and (c) are spectra comparisons at three different irradiation temperatures, indicating the irradiation dose dependence; (d) and (e) are spectra comparisons at two different irradiation doses, indicating the irradiation temperature dependence.

The measured positron lifetime spectra for neutron irradiated SiC were resolved into two lifetime components (one type of vacancy defect was considered). The results are plot in Figure 3. The short lifetime (fixed at 140 ps) indicates the positrons trapped in the SiC matrix. The long lifetime refers to the positrons annihilated in the vacancy defects. For the as-received SiC, the long lifetime of 230 ps indicates the presence of single Si-vacancy. For SiC samples irradiated at 380~440°C, the long lifetime (i.e., the size of the vacancy cluster) increases up to the radiation damage level of 0.11 dpa and then saturates in the damage range from 0.11 to 30 dpa, which implies that the size of the average vacancy cluster keeps constant. The lifetime of 275 ps indicates the presence of $(V_{Si})_3$ or $V_{Si}+V_C+V_{Si}$. On the other hand, the intensity of this long lifetime increases as the dose increases from 0.11 to 30 dpa, implying the increasing number density. The mean lifetime also shows a clearly increasing trend with increasing damage level. For SiC samples irradiated at 500~540°C, the long lifetimes for the two cases of 0.01 and 0.1 dpa are 263 and 265 ps, equivalent to the existence of $(V_C+ V_{Si})_2$, respectively. This value becomes 287 ps at 30 dpa, implying the existence of $(V_{Si})_4$ or $(V_{Si})_5$. Similar to the low temperature irradiation, the mean lifetime increases with increasing irradiation dose and is very close to that of low temperature irradiation. For high temperature irradiation, the long lifetime is greater than 300 ps at 1.4 dpa and 30 dpa, attributed to the existence of ring hexavacancy complex, $(V_C+V_{Si})_3$-ring, or larger silicon vacancy clusters. The mean lifetime is larger than the other two cases, indicating a more damaged microstructure. The corresponding intensities have a general increasing trend with increasing irradiation dose for all three irradiation temperatures.

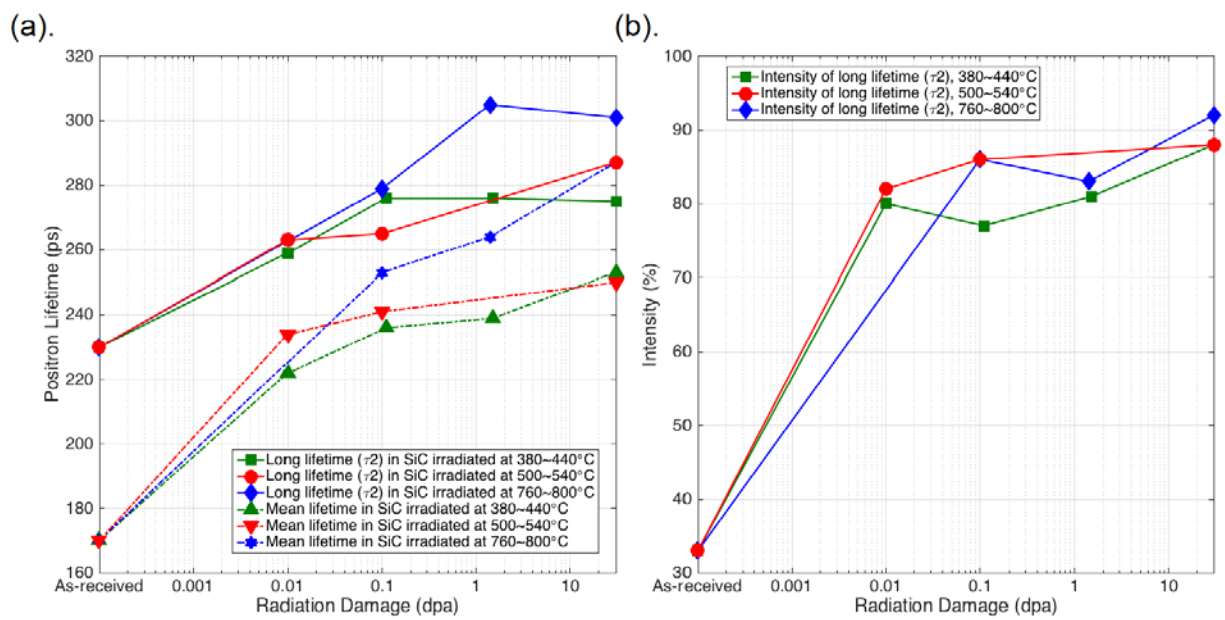

Figure 3. Positron lifetimes and the corresponding intensities as a function of radiation damage level for SiC irradiated at three different temperatures.

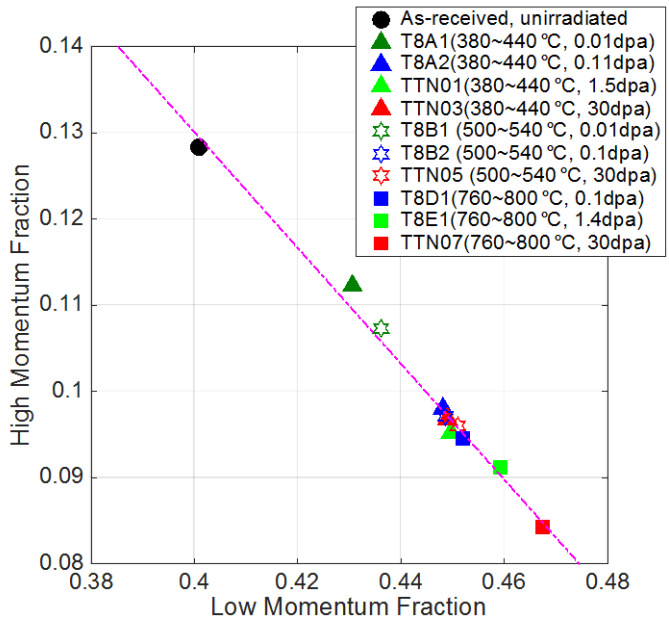

Figure 4. *S-W* plot for neutron irradiated SiC at various irradiation conditions. The dashed red line is drawn to guide the eye.

Figure 4 plots the S-W pairs obtained for various neutron irradiated SiC, demonstrating that there is no significant change in the defect nature in terms of defect distributions and types. S-W pairs for T8A2, TTN01, TTN03, T8B2, and TTN05 are quite close to each other, indicating the very similar vacancy clusters contained in these five samples, which is consistent with the positron lifetime analysis.

Future Work

More work is needed to analyze the vacancy cluster obtained from the PAS measurements in more details. The quantification of the vacancy clusters identified by PAS will be performed by applying the classic trapping model. The information of small vacancy clusters will then be linked to the measured swelling behavior of SiC subject to neutron irradiation, therefore, providing insight into the correlation between microstructure and the physical property of SiC.

References

[1] T. Koyanagi, K. Shimoda, S. Kondo, T. Hinoki, K. Ozawa, Y. Katoh, J. Nucl. Mater., 455 (2014) 73–80.
[2] T. Koyanagi, S. Kondo, T. Hinoki, J. Nucl. Mater., 442 (2013) S380–S383.
[3] Y. Katoh, N. Hashimoto, S. Kondo, L.L. Snead, A. Kohyama, J. Nucl. Mater., 351 (2006) 228–240.
[4] Y. Katoh, S. Kondo, L.L. Snead, J. Nucl. Mater., 382 (2008) 170–175.
[5] X. Hu, T. Koyanagi, M. Fukuda, Y. Katoh, L.L. Snead, B.D. Wirth, J. Nucl. Mater., 470 (2016) 278–289.
[6] X.L. Yang, W.X. Zhu, C.D. Wang, H. Fang, T.J. Yu, Z.J. Yang, G.Y. Zhang, X.B. Qin, R.S. Yu, and B.Y. Wang, Applied Physics Letters, 94(15) (2009) 151907.